Effect of sintering temperature and time on surface hardness of cold-pressed $SrFe_{12}O_{19}$ pellets: An orthogonal experimental approach

Mai Van Huy[1], To Thanh Loan[2], Tran Thi Viet Nga[2],
Nguyen Manh Tien[1], Tran Duc Hoan[1*]

[1]Le Quy Don Technical University, 236 Hoang Quoc Viet, Bac Tu Liem, Hanoi, Vietnam;
[2]School of Materials Science and Engineering, Hanoi University of Science and Technology, 1 Dai Co Viet, Hai Ba Trung, Hanoi, Vietnam.
[*]Corresponding author: tranduchoan@lqdtu.edu.vn
Received 28 Feb. 2025; Revised 16 Apr. 2025; Accepted 23 Apr. 2025; Published 25 Jun. 2025.
DOI: https://doi.org/10.54939/1859-1043.j.mst.104.2025.182-191

ABSTRACT

This study explores the influence of sintering temperature and time on the surface hardness and microstructure of cold-pressed $SrFe_{12}O_{19}$ permanent magnet compacts. A two-factor orthogonal experimental design was employed to construct a regression model with high predictive accuracy (R^2 = 97.23%, AICc = 55.14). Rietveld refinement of X-ray diffraction (XRD) data confirmed the formation of a single-phase of M-type hexagonal structure, with crystallite sizes ranging from 39.5 to 61.8 nm and microstrain values dependent on sintering conditions. The optimal hardness of 93.63 HV was obtained at 1000 °C for 120 minutes, closely matching the model prediction (95.287 HV) with a deviation of only 1.74%. The results demonstrate that controlling sintering parameters is crucial for minimizing microstrain and maximizing hardness, offering practical insights for the processing of high-performance ferrite-based magnetic ceramics.

Keywords: Strontium hexaferrite; Cold pressing; Sintering; Surface hardness; X-ray diffraction; Regression analysis.

1. INTRODUCTION

Strontium hexaferrite ($SrFe_{12}O_{19}$) is an M-type hexagonal ferrite that has gained considerable attention as a hard magnetic material due to its high coercivity, large magnetocrystalline anisotropy, excellent thermal and chemical stability, and moderate production cost. These features make $SrFe_{12}O_{19}$ highly suitable for use in electromagnetic devices such as motors, sensors, permanent magnets, and microwave absorbers [1]. While numerous studies have aimed to enhance the magnetic properties of $SrFe_{12}O_{19}$ through particle size refinement, phase purity improvement, and optimized sintering techniques, its mechanical performance, particularly surface hardness, has received comparatively little attention. In structural and functional applications, surface hardness plays a critical role in determining wear resistance, dimensional stability, and mechanical durability. This property is strongly influenced by microstructural features such as crystallite size, microstrain, and porosity, all of which are highly sensitive to sintering conditions [2].

To address the need for enhanced structural performance, various synthesis techniques such as sol-gel, auto-combustion, and mechanical milling, have been applied to produce nanostructured $SrFe_{12}O_{19}$ powders. For example, M. Stingaciu et al. demonstrated the importance of rapid consolidation and controlled nanocrystallite formation in enhancing magnetic performance [3]. Similarly, R. Suresh et al. investigated how changes in sintering temperature influence phase development and magnetic response [4]. The study by E. Ürögiová et al. indicated that the mechanical hardness of rubber–ferrite composites is highly dependent on the microstructural features of $SrFe_{12}O_{19}$, particularly particle morphology and filler dispersion [5]. This finding implies that the intrinsic mechanical behavior of $SrFe_{12}O_{19}$ must be better understood and optimized, especially in dense ceramic forms. Supporting this, Yat Choy Wong et al. found that increasing sintering temperature from 800 °C to 1000 °C improved phase purity and crystallinity, indicating that densification and grain structure evolution are key to performance [6]. In a related

study, A.U. Rashid et al. showed that crystallite size and morphology significantly affect magnetic losses, which are inherently tied to microstructure quality [7]. Despite these insights, there remains a lack of systematic studies focusing on how sintering temperature and time affect the surface hardness of $SrFe_{12}O_{19}$ ceramics. While some works have noted the influence of sintering on magnetic properties, the impact on mechanical performance, particularly from a process optimization perspective, has not been thoroughly investigated. Moreover, few studies employ statistical experimental design methods to evaluate and model these effects quantitatively.

In this study, we investigate the influence of synthesis conditions on the surface hardness of cold-pressed $SrFe_{12}O_{19}$ compacts. The strontium hexaferrite ($SrFe_{12}O_{19}$) powder employed was synthesized via the sol-gel method, a simple and cost-effective technique to prepare high-purity strontium hexaferrite. The sol-gel synthesis of $SrFe_{12}O_{19}$ was previously reported by Tran Thi Viet Nga et al. [8], who examined the effects of pH, Fe/Sr molar ratio, calcination temperature, and calcination time on phase formation and the magnetic properties of $SrFe_{12}O_{19}$. The research demonstrated that a single-phase $SrFe_{12}O_{19}$ was obtained at a calcination temperature of 950 °C with an Fe/Sr molar ratio of 10.5 and a solution pH of 1. Additionally, they confirmed that calcination temperature and duration significantly affect phase formation. The $SrFe_{12}O_{19}$ phase is formed at calcination temperatures of 850 °C. However, although calcination at 950 °C for 2 hours yielded nearly pure $SrFe_{12}O_{19}$, trace impurities (approximately 1%) of hematite and $Sr(NO_3)_2$ remained. This was attributed to the low packing density of the powder during heat treatment, which limited the complete reaction of the oxide phases to form a single-phase $SrFe_{12}O_{19}$. Therefore, in the present study, instead of directly calcining the powder after heating, we propose an improved approach by applying cold compaction to increase the packing density before calcination at various temperatures and durations. A two-level orthogonal experimental design is adopted to model the relationship between hardness and processing parameters, including calcination temperature and calcination time. The temperature range of 850 °C to 1000 °C was chosen to investigate since the previous studies showed that the $SrFe_{12}O_{19}$ phase can be fully formed in this temperature range [6, 8]. Higher temperatures (above 1000 °C) were not considered in order to avoid grain coarsening and excessive densification, which could degrade mechanical properties such as surface hardness and fracture resistance. Besides, the publications on the synthesis of strontium hexaferrite also indicated that calcination time in the range of 2 h to 5 h is sufficient for complete phase development, particularly in cold-pressed green bodies that require a longer holding time for diffusion and crystallization [7, 8]. Hence, the calcination time range of 120 min to 360 min was selected for investigation. Crystallographic and microstructural characteristics are analyzed using Rietveld refinement of X-ray diffraction (XRD) data, while regression modeling is used to identify optimal conditions. The findings provide new insight into how sintering conditions control surface hardness and offer guidance for developing $SrFe_{12}O_{19}$ materials with enhanced mechanical durability for practical applications.

2. MATERIALS AND METHODS

2.1. Materials

The precursor powder of strontium hexaferrite ($SrFe_{12}O_{19}$) was synthesized using the sol-gel route as previously described in the literature [8]. Specifically, $Fe(NO_3)_3$ (1M) and $Sr(NO_3)_2$ (1M) solutions were dissolved in deionized water with an Fe/Sr molar ratio of 10.5. Citric acid was subsequently added to the solution at a fixed $[Sr^{2+} + Fe^{3+}]$: $C_3H_4(OH)(COOH)_3$ molar ratio of 1:3. NH_4OH was used to adjust the pH within the range of 1 to 8. Once the pH was stabilized at 1, the solution was stirred at 1000 rpm and gradually evaporated at 80 °C. As the water evaporated, the remaining mixture transformed into a highly viscous brown gel. The gel was then dried at 100 °C for 24 h, and subsequently heated at 500 °C for 2 h.

2.2. Cold compaction

Approximately 0.6 g of the synthesized precursor powder of $SrFe_{12}O_{19}$ was loaded into a cylindrical die for cold pressing. The die assembly was installed on a YH-28 100-ton hydraulic press at the Metal Forming Laboratory, Le Quy Don Technical University, as shown in figure 1(a). During compaction, no specific pressure value or holding time was set. Instead, the compaction was carried out by moving the punch downward until it reached a fixed position to ensure the desired dimensions. After reaching this position, the punch was retracted upward, and the pressed $SrFe_{12}O_{19}$ pellet was ejected onto the die surface for removal. The resulting cylindrical pellets had dimensions of approximately 10 mm in diameter and 1.4 mm in thickness, with a dimensional tolerance of ± 0.05 mm, as illustrated in figure 1(b).

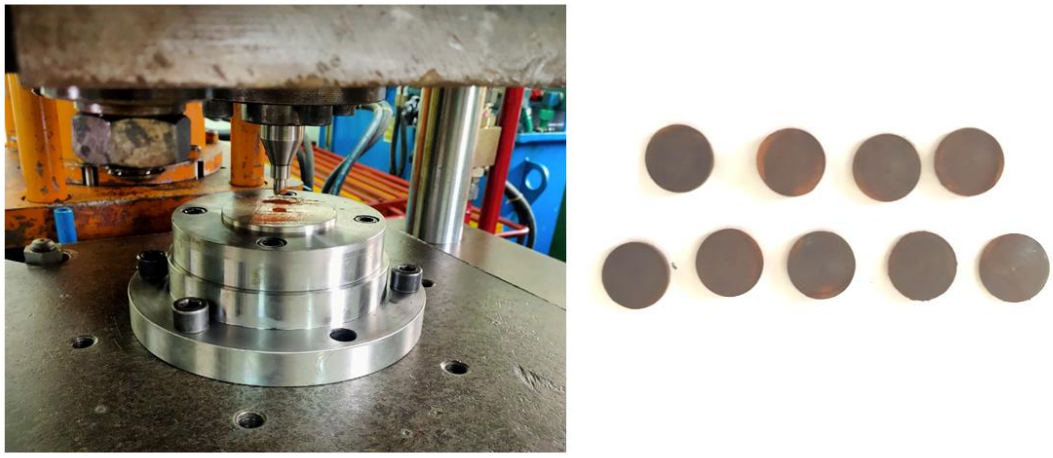

a) b)

Figure 1. *Experimental setup showing the die assembly mounted on the YH28-100 ton hydraulic press (a) and $SrFe_{12}O_{19}$ pellet samples after cold-pressing in the cylindrical mold (b).*

2.3. Sintering process

Sintering was carried out in an LH120/13 Nabertherm furnace under atmospheric conditions at the Metal Forming Laboratory, Le Quy Don Technical University. A two-factor, two-level full factorial design with four center-point replications ($2^2 + 4$) was employed to systematically investigate the effects of sintering temperature (850 – 1000 °C, coded as x_1) and sintering duration (120 – 360 minutes, coded as x_2) on the surface hardness of the cold-pressed $SrFe_{12}O_{19}$ pellets. The detailed layout of the experimental runs and corresponding surface hardness results are presented in table 1.

Table 1. *Sintering conditions and coded variables in the orthogonal experimental design.*

Sample	Sintering temp, ºC	Sintering time, min	x_1	x_2
S1	850	120	-	-
S2	1000	120	+	-
S3	850	360	-	+
S4	1000	360	+	+
S5	925	240	0	0
S6	925	240	0	0
S7	925	240	0	0
S8	925	240	0	0
Note: Experiments S5-S8 are replicated center points to evaluate curvature in the design				

2.4. Characterization

The X-ray diffraction (XRD) experiment was performed using the D2-Phaser diffractometer (Bruker) with a Cu anode (wavelength λ = 1.541838 Å) to determine the phase composition and crystal structure. The XRD data were analyzed using the Rietveld refinement method with FullProf software. The fitting quality was evaluated based on the χ^2 value and the R_{wp} factor, where the analysis results are considered reliable when χ^2 approaches 1 and R_{wp} is close to 10%.

The surface hardness of the sintered $SrFe_{12}O_{19}$ pellets was measured using a Vickers hardness tester (Wolpert Wilson 432SVD, Materials Laboratory, Le Quy Don Technical University). A constant load of 200 g was applied for 15 seconds during each indentation. For each sample, three independent measurements were taken at the central region of the pellet surface to minimize edge effects, and the average value was reported in units of Vickers Hardness (HV). The instrument was calibrated according to ISO 6507 standards. The standard deviation across all measurements remained within acceptable limits (± 2.0 HV0.2). These measurements formed the basis for evaluating the effects of sintering parameters on the mechanical properties, which were in line with the objectives of the orthogonal experimental design.

The morphology and the grain size of the investigated samples were observed via scanning electron microscopy (SEM, JEOL-JSM 7600F).

3. RESULTS AND DISCUSSION

3.1. Microstructural and crystallographic analysis by XRD

Figure 2 shows the XRD patterns of the precursor sample as well as the S1, S2, S3, and S4 samples. It can be observed that the precursor sample contains γ-Fe_2O_3 and $Sr(NO_3)_2$ phases because, after heating, the $SrFe_{12}O_{19}$ phase had not formed yet. Meanwhile, the characteristic diffraction peaks of the $SrFe_{12}O_{19}$ phase appeared in the samples after sintering.

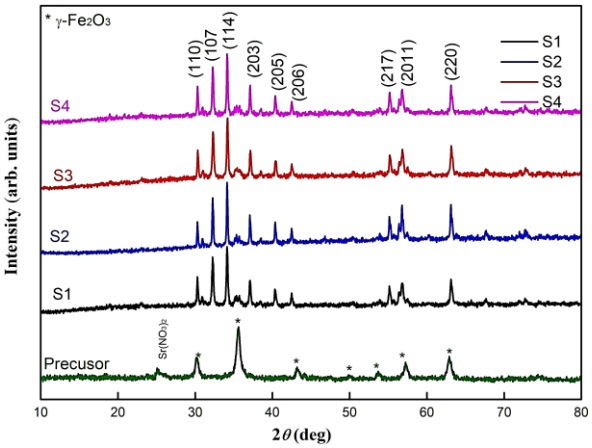

Figure 2. *XRD patterns of $SrFe_{12}O_{19}$ samples sintered under different conditions and the precursor sample.*

The Rietveld method was used to analyze the XRD data in detail to determine the information of the phase composition, crystal structure, and microstructure. Figure 3 displays the diffraction patterns and Rietveld analysis of the investigated samples. The refinement results show that the samples are completely single-phase of $SrFe_{12}O_{19}$ with a hexagonal structure belonging to the $P6_3/mmc$ space group. The parameters obtained from the Rietveld analysis, including lattice parameters (a, c), unit cell volume (V), and microstructure parameters, are listed in table 2. The microstructure parameters, including crystal size (D_{XRD}) and microstrain (ε), were determined simultaneously with other structural parameters in the Rietveld analysis based on the broadening of

the diffraction peaks. In the peak broadening analysis, the instrumental resolution function derived from the peak broadening of the standard Al_2O_3 sample was provided. The peak broadening due to crystallite size and microstrain was determined after subtracting the instrumental broadening.

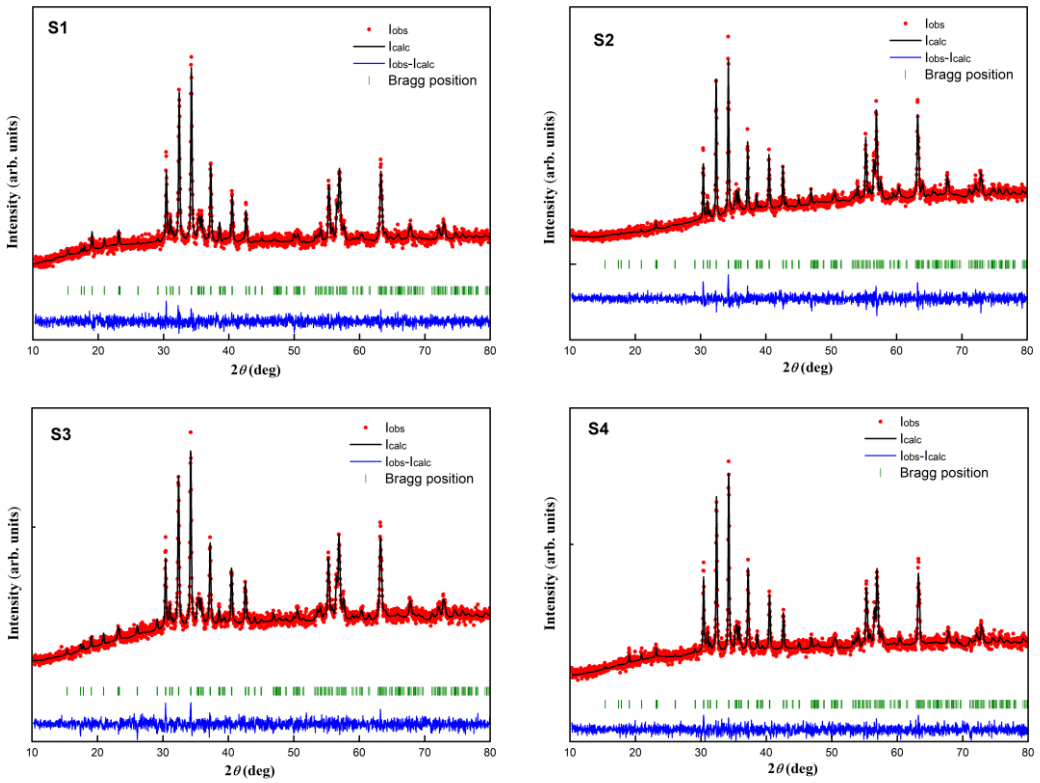

Figure 3. *Rietveld refinement analyses of the S1, S2, S3, and S4 samples. The experimental points (red points), as well as calculated (black line) and difference functions (blue line), are indicated. The green marks indicate the Bragg positions of the diffraction peaks.*

Since a unit cell of $SrFe_{12}O_{19}$ contains two formula units, the mass density of the samples was identified via the relation:

$$\rho_{XRD} = \frac{2M}{N_A V} \tag{1}$$

Where M is the mole mass in grams of $SrFe_{12}O_{19}$ (M = 1061.76 g), N_A is the Avogadro constant, and V is the unit cell volume estimated from Rietveld analyses as presented in table 2. The calculated mass density values are also presented in table 2. The obtained mass density values of the samples are higher than the theoretical density calculated for $SrFe_{12}O_{19}$ (ρ_{theory} = 5.1 g/cm^3 [13]).

Table 2. *Results of Rietveld analyses of the $SrFe_{12}O_{19}$ samples: lattice parameters (a, c), unit cell volume (V), average crystallite size (D_{XRD}), and microstrain (ε).*

Sample	*a*, Å	*c*, Å	*V*, Å^3	D_{XRD}, *nm*	ε,%	Mass density, g/cm^3
S1	5.87577	23.03344	688.682	46	0.0935	5.12011
S2	5.87638	23.03449	688.857	61.8	0.0734	5.11881
S3	5.87719	23.03831	689.161	39.5	0.0823	5.11655
S4	5.877	23.03694	689.074	60.7	0.0733	5.11719

3.2. Experimental results and surface hardness model

The measured Vickers hardness values for the sintered samples under different conditions are summarized in table 3.

Table 3. *Surface hardness results of $SrFe_{12}O_{19}$ samples under different sintering conditions.*

Sample	S1	S2	S3	S4	S5	S6	S7	S8
Hardness, HV	88.3	93.1	51.6	65.4	72.3	75.3	76.8	73.5

Using regression analysis and applying the Corrected Akaike Information Criterion (AICc) for model selection, we obtained the optimal regression model as follows:

$$HV = 74.537 + 4.65x_1 - 16.1x_2 \quad (2)$$

$$HV = 49.4 + 0.062\ Temp - 0.1342\ Time \quad (3)$$

The selected model has an AICc value of 55.14, a high coefficient of determination (R^2 = 97.23%), and an adjusted R^2(adj) of 96.12%, indicating strong reliability and a good fit with the experimental data. The detailed Analysis of Variance (ANOVA) for this model is shown in table 4:

Table 4. *Analysis of variance.*

Source	DF	Adj SS	Adj MS	F-Value	P-Value
Model	2	1123.33	561.66	87.63	0.000
Linear	2	1123.33	561.66	87.63	0.000
Temp	1	86.49	86.49	13.49	0.014
Time	1	1036.84	1036.84	161.76	0.000
Error	5	32.05	6.41		
Curvature	1	0.03	0.03	0.00	0.953
Lack-of-Fit	1	20.25	20.25	5.16	0.108
Pure Error	3	11.77	3.92		
Total	7	1155.38			

The ANOVA results presented in table 3 indicate that the regression model is statistically significant, with a model F-value of 87.63 and a corresponding p-value less than 0.001. This confirms that the model provides a strong fit to the experimental data. The individual contributions of the sintering parameters were also assessed. Among the two main effects, sintering time (x_2) exhibited the most significant influence on surface hardness, with an extremely high F-value of 161.76 and a p-value of 0.000. This result highlights the strong sensitivity of $SrFe_{12}O_{19}$ compacts to sintering duration, where prolonged holding time can negatively affect densification and microstructure. In contrast, sintering temperature (x_1) also contributed significantly, albeit to a lesser extent, with an F-value of 13.49 and a p-value of 0.014. This indicates that while increasing temperature generally enhances surface hardness, its effect is less dominant than that of time.

The curvature test returned a very low F-value (0.00) and a high p-value (0.953), suggesting that the linear model adequately captures the relationship between the factors and the response within the studied range. Additionally, the lack-of-fit test yielded a p-value of 0.108, which is above the 0.05 significance level, indicating that the model's residuals are within acceptable limits and that the model does not suffer from systematic errors. Overall, the ANOVA analysis confirms that the model is statistically reliable and that both sintering parameters play essential roles in determining the surface hardness of $SrFe_{12}O_{19}$, with sintering time being the more influential factor.

3.3. Influence of sintering conditions on surface hardness

The influence of sintering parameters on the surface hardness of cold-pressed $SrFe_{12}O_{19}$ compacts was further examined through statistical visualization and correlation with microstructural changes. As shown in the main effects plot (figure 4), increasing the sintering temperature from 850 °C to

1000 °C resulted in a significant increase in surface hardness. At the shortest sintering duration (120 minutes), hardness increased markedly, reaching a maximum of 93.1 HV at 1000 °C. This trend is attributed to enhanced diffusion and densification during high-temperature sintering, which improves particle bonding, reduces porosity, and promotes better crystallite development. The Rietveld refinement results support this explanation, with sample S2 (1000 °C, 120 min) showing the largest crystallite size (61.8 nm) and the lowest microstrain (7.34%).

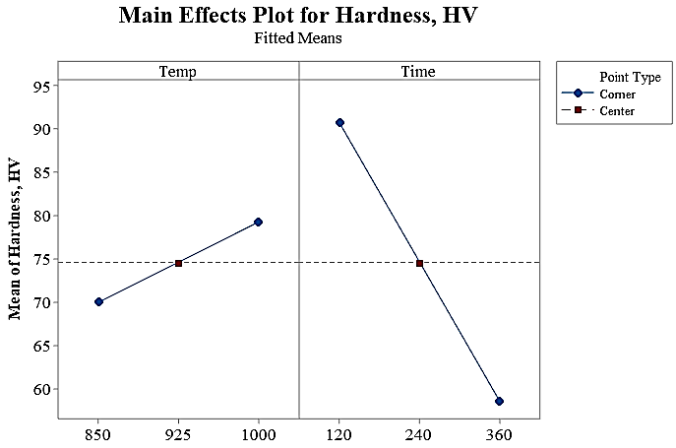

Figure 4. *Main effects plot for sintering temperature and time on the surface hardness of $SrFe_{12}O_{19}$ samples.*

The SEM image of the S2 sample, presented in figure 5, reveals that the grain size varies between 50 and 100 nm. This observation is consistent with the crystallite size estimated from XRD. The grain size of this sample is similar to that of strontium ferrite powders synthesized entirely by the sol-gel method under identical conditions and calcined at 850 °C, as previously reported by Tran Thi Viet Nga *et al.*[8]. This indicates that, within the investigated range of time and temperature, the synthesis conditions do not significantly affect the grain size. Additionally, these findings align with those of Azizah Wahi et al. in the study [9], where increased sintering temperature led to higher densification and surface hardness. Similarly, Marian Stingaciu et al., in [3], reported that sintering at optimal temperature improved crystallization, resulting in enhanced magnetic and mechanical performance of $SrFe_{12}O_{19}$.

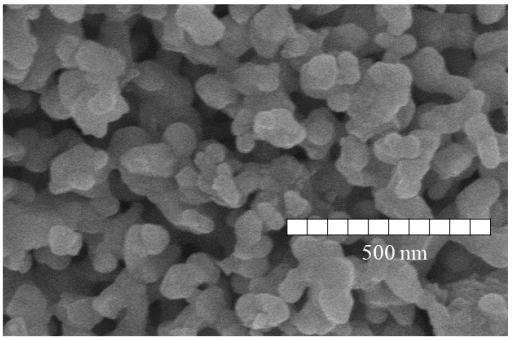

Figure 5. *SEM image of the S2 sample.*

Conversely, increasing the sintering time from 120 to 360 minutes had a negative effect on surface hardness. As seen in both the main effects and contour plots (figure 6), extended durations led to a substantial drop in hardness values. This reduction is likely caused by over-sintering, which induces excessive grain growth, microstructural coarsening, and higher internal strain. These effects are consistent with observations by Aftab et al. in [10], where prolonged thermal exposure increased microstrain and reduced mechanical integrity. Furthermore, Sriraman et al. emphasized

in [11] that reducing internal strain is essential for achieving higher hardness, a conclusion that aligns well with the present study's findings. In addition, microstructural degradation due to excessive sintering was also reported by Tran Thi Viet Nga and Nguyen Thi Lan in their study [12], where inappropriate sintering led to grain coalescence and lower mechanical stability. A similar trend was observed by Navin Kumar et al. in [14], where prolonged sintering deteriorated hardness due to strain accumulation and interface degradation.

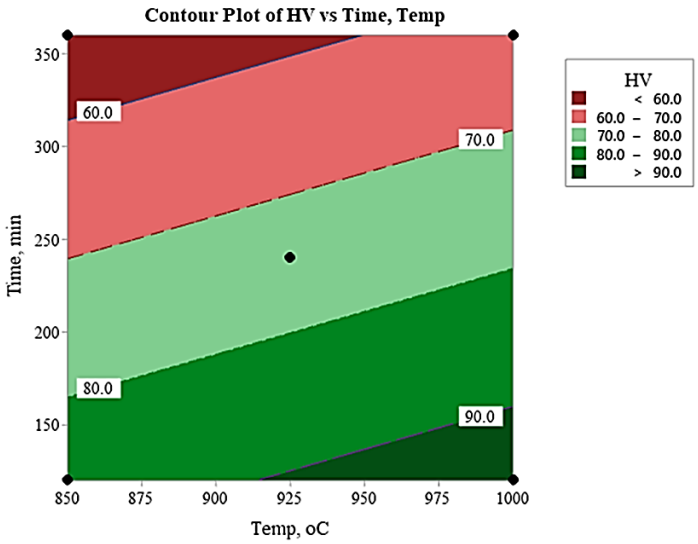

Figure 6. *Contour plot illustrating the effect of sintering temperature and time on the surface hardness of $SrFe_{12}O_{19}$ compact samples.*

The contour plot (figure 6) highlights the combined influence of temperature and time, identifying an optimal processing window for achieving maximum surface hardness. The highest values are concentrated at high temperatures and short sintering times, while lower values occur at long durations and low temperatures. These results confirm that balancing sintering parameters is critical to avoid microstructural instability and achieve desirable mechanical performance. Sample S2 represents the optimal sintering condition, combining high crystallinity, low microstrain, and the highest surface hardness. The alignment of these factors underpins the importance of carefully optimizing sintering schedules to control microstructure and enhance the mechanical behavior of $SrFe_{12}O_{19}$ materials.

3.4. Optimization of sintering conditions for maximum surface hardness

The optimal sintering conditions for achieving the highest surface hardness were identified based on the regression model developed in section 3.2. According to the model, the combination of a sintering temperature of 1000 °C and a sintering duration of 120 minutes yielded the maximum predicted surface hardness of 95.287 HV. To validate this prediction, a confirmation experiment was performed under these optimized conditions. The surface hardness was measured at the central region of the pellet using three independent indentations. The measured values were 92.8 HV, 93.6 HV, and 92.5 HV, resulting in an average of 93.63 HV. This closely matched the predicted value, with a relative deviation of only 1.74%, confirming the model's reliability and predictive accuracy. This strong agreement between the predicted and experimental results demonstrates that the regression model effectively captures the influence of sintering parameters on the surface hardness of $SrFe_{12}O_{19}$ compacts. Furthermore, it highlights the practical significance of optimizing the sintering profile, as even modest variations in temperature or time can lead to substantial changes in microstructure and, consequently, mechanical performance.

The optimized conditions established in this study provide a solid basis for the future processing

of $SrFe_{12}O_{19}$-based materials, especially in applications requiring consistent surface hardness and structural integrity. These findings emphasize that precise control of sintering parameters is essential not only for achieving high mechanical strength but also for ensuring reproducibility in the manufacturing of ceramic magnetic components.

4. CONCLUSIONS

This study examined the effects of sintering temperature and time on the surface hardness and microstructural evolution of cold-pressed $SrFe_{12}O_{19}$ samples. XRD and Rietveld analyses confirmed that all specimens retained a single-phase hexagonal structure, with variations in crystallite size and microstrain directly influenced by sintering parameters. Increasing the temperature led to grain growth and reduced strain, thereby enhancing surface hardness, while prolonged sintering time had a detrimental effect, likely due to over-sintering, increased internal stress, and degradation of microstructural cohesion. A statistically robust regression model (R^2 = 97.23%) revealed that sintering time had a stronger impact on hardness than temperature, highlighting the sensitivity of $SrFe_{12}O_{19}$ to thermal exposure duration.

The optimal sintering condition—identified as 1000 °C for 120 minutes—resulted in the highest crystallinity and lowest microstrain, yielding a predicted hardness of 95.287 HV and a measured average of 93.63 HV, with only 1.74% deviation. These findings demonstrate the importance of precisely controlling sintering parameters to balance densification and structural integrity. The proposed methodology offers a practical framework for optimizing the mechanical performance of $SrFe_{12}O_{19}$-based materials and may serve as a useful reference for the processing of other hard ferrite ceramics in magnetic and structural applications.

Acknowledgements: *This research is funded by Vietnam National Foundation for Science and Technology Development (NAFOSTED) under grant number 103.02-2023.60.*

REFERENCES

[1]. M. Stingaciu, M. Topole, P. McGuiness, and M. Christensen, *"Magnetic properties of ball-milled SrFe12O19 particles consolidated by Spark-Plasma Sintering,"* Sci. Rep., vol. 5, pp. 1–8, (2015), doi: 10.1038/srep14112.

[2]. Widyastuti, E. Kharismawati, M. Zainuri, and H. Ardhyananta, *"Microstructure and magnetic properties of barium hexaferrite produced by sol gel auto combustion for radar absorber material (RAM) application,"* Appl. Mech. Mater., vol. 493, pp. 656–660, (2014), doi: 10.4028/www.scientific.net/AMM.493.656.

[3]. M. Stingaciu, A. Z. Eikeland, F. H. Gjørup, S. Deledda, and M. Christensen, *"Optimization of magnetic properties in fast consolidated SrFe12O19 nanocrystallites,"* RSC Adv., vol. 9, no. 23, pp. 12968–12976, (2019), doi: 10.1039/c9ra02440a.

[4]. K. V. Suresh, P. Fernandes, and K. Raju, *"Investigation on performance and emission characteristics of diesel engine with cardanol based hybrid bio-diesel blends,"* Mater. Today Proc., vol. 35, no. xxxx, pp. 378–382, (2019), doi: 10.1016/j.matpr.2020.02.691.

[5]. E. Urogiova, I. Hudec, D. Bellusova, and Bratislava, *"Magnetic and Mechanical Properties of Strontium Ferrite – Rubber Composites,"* Test. Meas., no. 5, pp. 224–228, (2006).

[6]. Y. C. Wong, J. Wang, and G. B. Teh, *"Structural and magnetic studies of SrFe12O19 by sol-gel method,"* Procedia Eng., vol. 76, pp. 45–52, (2014), doi: 10.1016/j.proeng.2013.09.246.

[7]. A. U. Rashid, P. Southern, J. A. Darr, S. Awan, and S. Manzoor, *"Strontium hexaferrite (SrFe12O19) based composites for hyperthermia applications,"* J. Magn. Magn. Mater., vol.344, pp. 134–139, (2013), doi: 10.1016/j.jmmm.2013.05.048.

[8]. T. T. V. Nga, N. P. Duong, T. T. Loan, and T. D. Hien, *"Key step in the synthesis of ultrafine strontium ferrite powders (SrFe12O19) by sol-gel method,"* J. Alloys Compd., vol.610, pp. 630–634, (2014), doi: 10.1016/j.jallcom.2014.04.193.

[9]. A. Wahi, N. Muhamad, A. B. Sulong, and R. N. Ahmad, *"Effect of sintering temperature on density, hardness and strength of MIM Co30Cr6Mo biomedical alloy,"* Funtai Oyobi Fummatsu Yakin/Journal Japan Soc. Powder Powder Metall., vol. 63, no. 7, pp. 434–437, (2016), doi: 10.2497/jjspm.63.434.

[10]. M. Aftab, A. Aftab, M. Z. Butt, D. Ali, F. Bashir, and S. S. Iqbal, *"Surface hardness of pristine and laser-treated zinc as a function of indentation load and its correlation with crystallite size valued by Williamson-Hall analysis, size-strain plot, Halder-Wagner and Wagner-Aqua models,"* Mater. Chem. Phys., vol. 295, p. 127117, (2023), doi: 10.1016/j.matchemphys.2022.127117.

[11]. K. R. Sriraman, S. Ganesh Sundara Raman, and S. K. Seshadri, *"Influence of crystallite size on the hardness and fatigue life of steel samples coated with electrodeposited nanocrystalline Ni-W alloys,"* Mater. Lett., vol. 61, no. 3, pp. 715–718, (2007), doi: 10.1016/j.matlet.2006.05.049.

[12]. T. T. Viet Nga and N. T. Lan, *"Fabrication and exchange-spring properties of SrFe12O19@Fe3O4 nanocomposites with core-shell structure,"* Mater. Chem. Phys., vol.251, p. 123084, (2020), doi: 10.1016/j.matchemphys.2020.123084.

[13]. Marian Stingaciu et al., *"Optimization of magnetix properties in fast consolidated SrFe12O19 nanocrystallites,"* RSC Adv., vol. 9, pp. 12968-12976, (2019), doi: 10.1039/c9ra02440a

[14]. N. Kumar et al., *"Optimization of Sintering Process Parameters by Taguchi Method for Developing Al-CNT-Reinforced Powder Composites,"* Crystals, vol. 44, no. 9, pp. 5924–5933, (2023), doi: 10.1002/pc.27537.

TÓM TẮT

Ảnh hưởng của nhiệt độ và thời gian thiêu kết đến độ cứng bề mặt của viên nén $SrFe_{12}O_{19}$ ép nguội: một cách tiếp cận thực nghiệm trực giao

Nghiên cứu này khảo sát ảnh hưởng của nhiệt độ và thời gian thiêu kết đến độ cứng bề mặt và vi cấu trúc của các viên nén $SrFe_{12}O_{19}$ ép nguội, được sử dụng làm nam châm vĩnh cửu. Thiết kế thí nghiệm trực giao hai yếu tố đã được áp dụng để xây dựng mô hình hồi quy với độ chính xác dự đoán cao (R^2 = 97,23%, AICc = 55,14). Phân tích Rietveld từ dữ liệu nhiễu xạ tia X (XRD) xác nhận sự hình thành pha đơn của cấu trúc lục giác kiểu M, với kích thước tinh thể dao động từ 39,5 đến 61,8 nm và độ biến dạng vi mô phụ thuộc vào các điều kiện thiêu kết. Độ cứng bề mặt tối ưu đạt 93,63 HV ở 1000 °C trong 120 phút, rất gần với giá trị dự đoán từ mô hình (95,287 HV) với độ lệch chỉ 1,74%. Kết quả này cho thấy việc kiểm soát các thông số thiêu kết đóng vai trò quan trọng trong việc giảm thiểu độ biến dạng vi mô và tối đa hóa độ cứng, cung cấp các hiểu biết thực tiễn cho quá trình xử lý gốm từ $SrFe_{12}O_{19}$ hiệu suất cao.

Từ khoá: Strontium hexaferrite; Ép nguội; Thiêu kết; Độ cứng bề mặt; Nhiễu xạ tia X; Phân tích hồi quy.